On the Possibility of Detecting Low Barrier Hydrogen Bonds with Kinetic Measurements

Nolan E. Dean, Jeffrey E. Miller, Christopher J. Halkides, and Michael Messina*

Department of Chemistry, University of North Carolina, Wilmington, Wilmington, North Carolina 28403

Received October 14, 2002

Recent experimental evidence has pointed to the possible presence of a short, strong hydrogen bond in the enzyme−substrate transition states in some biochemical reactions. To date, most experimental measures of these short, strong hydrogen bonds have monitored their equilibrium properties. In this work we show that kinetic measurements can also be used to detect the presence of short, strong hydrogen bonds. In particular, we find nontrivial differences among rate constant ratios of protonated to deuterated hydrogen bonds between strong and weak hydrogen bonds for proton transfer between donor−acceptor sites. We quantify this kinetic isotope effect by performing dynamical calculations of these rate constants by computing reactive flux through a dividing surface. This reactive flux is computed by evolving trajectories on an effective quantum mechanical potential energy surface.

I. INTRODUCTION

The presence of short, strong hydrogen bonds is now believed to be an important structural property in transition states of some biochemical reactions. These strong hydrogen bonds between an enzyme and substrate in a biochemical pathway are termed low barrier hydrogen bonds (LBHB) and are believed to increase rates of these biochemical reactions by orders of magnitude.[1−10]

The most common methods used to detect the presence of these LBHBs are thermodynamic in nature and thus probe their equilibrium properties. One measure is the isotopic fractionation factor, which is the equilibrium constant for the reaction in which the proton involved in a LBHB is replaced by a deuteron.[7] Other experimental techniques used to detect the presence of LBHBs rely on spectroscopy such as X-ray diffraction,[9] NMR,[10] and IR.[11] These techniques also probe the equilibrium properties of the LBHB.[5] In this work we show that it is possible to detect the presence of a LBHB through kinetic measurements of proton and deuteron transfer between the donor and acceptor sites in a molecule containing a hydrogen bond.

The potential energy surface governing the LBHB is well represented as a double-well potential. The minima of the potential represent states where the proton (or deuteron) is localized on the donor or acceptor moieties in a molecule. The barrier between the minima represents the energetic barrier that must be overcome for the proton to transfer between donor and acceptor sites.

As mentioned above, the value of the isotopic fractionation factor is very useful for detecting the presence of LBHB. This fractionation factor is essentially the ratio of partition functions for deuterated to protonated species. Since, in the equilibrium case, the ratio of thermodynamic properties of protonated to deuterated hydrogen bonds can be useful in detecting the presence of LBHBs, it is reasonable to expect such variations will exist between the rate constants. Further, such kinetic isotope effects are well-known throughout chemistry and have been exploited experimentally for some time.

The goal of this work is to quantify as rigorously as possible what kinetic isotope effects to expect in a proton transfer between donor and acceptor sites in a hydrogen bond. In particular, to quantify how this isotope effect varies with hydrogen bond strength. To this end we compute rate constants for systems containing weak and strong LBHBs using trajectories to compute the reactive flux through a dividing surface.

Since the critical reaction coordinate involves the low-mass proton (and deuteron), quantum mechanical effects are extremely important and must be included in the calculation of the rate constants. We include quantum effects by propagating the trajectories on an effective quantum mechanical potential energy surface. In a previous work by one of us, we have shown that such an approach compares very favorably to the analogous exact quantum mechanical calculations based on the flux correlation function.[12]

It is well-known that a rate constant for proton transfer in an isolated double-well potential does not exist. This is because no species below the barrier has any way to overcome the energetic barrier, and all species with energy above the barrier will perpetually shuttle back and forth between reactants and products. The only way for a proton (deuteron) to successfully transfer from the donor to the acceptor site is for it to be coupled to external degrees of freedom that can act as a source or sink of energy.

In this work we couple the LBHB proton coordinate to a set of harmonic oscillators. The frequencies and couplings of these harmonic oscillators are chosen from a mapping of the Generalized Langevin Equation[13] (GLE) to a system coordinate coupled to a discrete set of oscillators. We compute the ratio of rate constants for deuteron to proton transfer in several double-well potentials which represent varying strengths of an intramolecular hydrogen bond. We

* Corresponding author phone: (910)962-7298; fax: (910)962-3013; e-mail: messinam@uncwil.edu.

10.1021/ci0203444 CCC: $25.00
Published on Web 01/17/2003

will couple this proton LBHB coordinate to several different sets of harmonic oscillators each representing a variety of friction strengths and time-scales of solvent response.

This paper is organized as follows: in section II we present the equations needed to compute the reactive flux on an effective quantum mechanical potential energy surface. In section III we present numerical results and in section IV we conclude.

II. REACTIVE FLUX ON EFFECTIVE QUANTUM POTENTIAL ENERGY SURFACE

The classical formulation of rate theory gives a well-defined definition of the rate constant as a reactive flux through a dividing surface separating reactants from products. Within the classical formulation, the rate constant, κ, is proportional to the plateau value of the reactive flux correlation function $C(\tau)$.[14]

$$C(\tau) = Q_R\kappa \tag{1}$$

Here Q_R is the reactant partition function and τ is a time large enough for the correlation function to reach a plateau value. The classical expression for this correlation function is

$$C(t) = \int d\vec{x}_o d\vec{p}_o e^{-\beta H(\vec{x}_o,\vec{p}_o)}\delta[Z]\dot{Z}\chi(\vec{x}(t),\vec{p}(t);\vec{x}_o,\vec{p}_o) \tag{2}$$

The set $\{\vec{x}_o,\vec{p}_o\}$ is the set of initial conditions, Z is the functional form of the dividing surface separating products and reactants, and $\dot{Z}$ is the time derivative of Z. This time derivative is defined by the Poisson bracket of Z and the system Hamiltonian, $H(x,p)$.

$$\dot{Z} = \{H,Z\} \tag{3}$$

The characteristic function $\chi(\vec{x}(t),\vec{p}(t);\vec{x}_o,\vec{p}_o)$ is the dynamic component of the correlation function and keeps track of which trajectories are on the product side of the dividing surface at time, t. We take β as the inverse temperature, $\beta = (1/kT)$, with k the Boltzmann constant.

The potential energy of our system is given by

$$V(x,\vec{y}) = V_{\mathrm{LBHB}}(x) + \frac{m}{2}\sum_j^N \omega_j^2(y_j - c_j x)^2 \tag{4a}$$

$$V_{\mathrm{LBHB}}(x) = Ax^4 - Bx^2 + D \tag{4b}$$

Here V_{LBHB} is the double-well potential along the proton coordinate, x, of the LBHB.[15] The height of the barrier is given by D, and it is related to A and B through $D = (B^2/4A)$. This is a symmetric double well. We acknowledge here that it is not possible to experimentally differentiate between the donor and acceptor sites in the symmetric double well potential. Thus, an experimental value for the rate constant for transfer between these two sites cannot be measured in a symmetric system. We use the symmetric double well, in this work because it is simpler, and the goal of this work is to quantify the order of magnitude of the isotope effect in hydrogen bonded systems. We have found that slight asymmetries in the potential do not appreciably change the results.

The coordinates $\{\vec{y}\}$ represent the set of N harmonic oscillators that couple to the LBHB coordinate. The frequencies, ω_j, and coupling, c_j, of these N oscillators are chosen from the well-known mapping of the GLE.[13,16] In a previous work one of us has shown that an effective quantum mechanical potential can be defined as[17]

$$V(x,\vec{y}) = V_{\mathrm{classical}}(x,\vec{y}) - \frac{1}{\beta}\ln\{W(x)\} \tag{5}$$

Here $W(x)$ is a weight function given by

$$W(x) = \prod_j^{N+1} \frac{\hbar\beta\sqrt{\lambda_j(x)}}{2\sinh\left(\frac{\hbar\beta\sqrt{\lambda_j(x)}}{2}\right)} \tag{6}$$

The $\{\lambda_j(x)\}$ are the eigenvalues of the force constant matrix whose elements are

$$[\mathbf{V}]_{11} = \frac{\partial^2 V}{\partial x^2} = 12Ax^2 - 2B + \sum_j \omega_j^2 c_j^2 \tag{7a}$$

$$[\mathbf{V}]_{1j} = \frac{\partial^2 V}{\partial x \partial y_j} = -\omega_j^2 c_j \tag{7b}$$

$$[\mathbf{V}]_{kk} = \frac{\partial^2 V}{\partial y_k \partial y_k} = \omega_k^2 \tag{7c}$$

If an eigenvalue is less than zero we treat the system coordinate, x, as a truncated parabolic barrier at point x.[18] Then the weight function takes a different form than in eq 6 and this is discussed in refs 17 and 18.

Since the force constant matrix is independent of the bath coordinates, $\vec{y}$, the weight function, in this case, only depends on the hydrogen bond coordinate, x. The independence of the weight function from the bath coordinates is very convenient. Generally, if one needs to propagate classical trajectories on a potential surface, the first derivative of this surface must be computed along each degree of freedom at each time step. This becomes very inefficient when the effective quantum mechanical potential depends explicitly on $\{\vec{y}\}$ since there is no simple analytical expression for the first derivative of the effective quantum potential surface. In the case above, the bath part of the effective quantum potential is identical to the classical potential and the spatial first derivatives along these degrees of freedom are trivial to compute. We find it most efficient to fit the $V_{\mathrm{LBHB}}(x)$ part of the effective potential to a quadratic-quartic potential with new, effective values of A and B

$$V_{\mathrm{LBHB}}^{\mathrm{eff}}(x) = A_{\mathrm{eff}}x^4 - B_{\mathrm{eff}}x^2 + D_{\mathrm{eff}} \tag{8}$$

where A_{eff} and B_{eff} are new A and B parameters needed to reproduce the effective quantum potential along the x degree of freedom. The new barrier height is D_{eff} and is given by $D_{\mathrm{eff}} = (B_{\mathrm{eff}}^2/4A_{\mathrm{eff}})$. We will see that the new, effective barrier height is reduced from the classical potential and thus reflects the tunneling and zero-point energy corrections.

Classically, eq 2 for the reactive flux is independent of the form and placement of the dividing surface. This is not

strictly true in the case of the propagation of classical trajectories on an effective quantum mechanical potential, but we have found, numerically, that the rate constant depends very weakly on the choice of the dividing surface.[12] We choose to put the dividing surface at $x = 0$ (i.e., $Z = x = 0$). With this choice of dividing surface and the effective quantum potential substituted for the original potential, the expression in eq 2 becomes

$$C(t) = e^{-\beta D_{\text{eff}}} \int dp_{xo} d\vec{y}_o d\vec{p}_{yo} \frac{p_{xo}}{\mu} e^{-\beta H_{\text{eff}}(x_0=0, p_{xo}, \vec{y}_o, \vec{p}_{yo})} \chi_{\text{eff}}(t) \tag{9}$$

Here, $\chi_{\text{eff}}(t)$ is the characteristic function as computed by running trajectories on the effective quantum potential surface.

The reactant partition function is obtained by evaluating matrix element V_{11} in eq 7a at the well minima so V_{11} becomes $4B + \sum_j \omega_j^2 c_j^2$. The force constant matrix is diagonalized yielding a set of eigenvalues $\{\lambda_j\}$. The reactant partition function is then given by

$$Q_R = \prod_{j=1}^{N+1} \frac{1}{2\sinh\left\{\hbar\beta\frac{\sqrt{\lambda_j}}{2}\right\}} \tag{10}$$

The ratio of deuterated to protonated rate constants can now be written as

$$\frac{\kappa_D}{\kappa_H} = \left(\frac{Q_R^H}{Q_R^D}\right) e^{-\beta(D_{\text{eff}}^D - D_{\text{eff}}^H)} \frac{\langle\chi_{\text{eff}}\rangle_D}{\langle\chi_{\text{eff}}\rangle_H} \tag{11}$$

Here $\langle\chi_{\text{eff}}\rangle$ denotes the value of the integral in eq 9 at the plateau time, τ. The ratio of partition functions for protonated to deuterated species, i.e., $((Q_R^H/Q_R^D))$ in eq 11, can be written as the inverse of the isotopic fractionation factor, φ.

$$\frac{\kappa_D}{\kappa_H} = \left[\frac{e^{-\beta(D_{\text{eff}}^D - D_{\text{eff}}^H)}}{\varphi}\right]\left(\frac{\langle\chi_{\text{eff}}\rangle_D}{\langle\chi_{\text{eff}}\rangle_H}\right) \tag{12}$$

The first term in eq 12 contains all the thermodynamic components of the rate constant ratio, while the second term contains the dynamic component.

III. NUMERICAL RESULTS

Calculations of the rate constant ratios from eq 12 are performed in two steps. In the first step we determine all the thermodynamic information in eq 12. The effective quantum potentials are computed via eqs 5−7 for several different bath frictions, time scales, and two LBHB potential energies, $V_{\text{LBHB}}(x)$. We consider a LBHB with A parameter and B parameters given by 0.07 au and 0.04 au, respectively. This set of parameters leads to a low barrier height of 15 kJ mol^{-1} and thus is indicative of a strong hydrogen bond. We also consider a weak hydrogen bond system with A and B parameters given by 0.07 au and 0.1 au, respectively. This leads to a large barrier of 94 kJ mol^{-1} and thus models a weak hydrogen bond.

We consider two friction time scales, slow and fast. The slow friction has a time constant of $\sigma = 800$ fs, and the fast friction has $\sigma = 3000$ fs [for details see eqs 6−10 of ref 16]. The rate constants exhibit the classical Kramers turnover behavior with respect to friction strength. We will refer to weak friction as friction values before the turnover region and strong friction as friction values after the turnover region.

We compute the effective quantum potentials for each friction strength and time scale according to eq 5 and then fit the effective quantum potentials, $V_{\text{LBHB}}(x)$, to a quadratic-quartic functional form with new values of A and B (i.e., A_{eff} and B_{eff}) in eq 8.

The ratio of deuterated to protonated partition functions yields the isotopic fractionation factor, φ, in eq 12. We computed these partition functions with eq 10 with the V_{11} matrix element is evaluated at the well minima as described above.

The second part of the calculations involves the computation of the dynamical component of this ratio. To compute this dynamical component we must compute the plateau value of the following

$$\langle\chi_{\text{eff}}\rangle = \int dp_{x_o} d\vec{y}_o d\vec{p}_{y_o} \frac{p_{xo}}{\mu} e^{-\beta H_{\text{eff}}(x_0=0, p_{xo}, \vec{y}_o, \vec{p}_{yo})} \chi_{\text{eff}}(t) \tag{13}$$

We do this by running classical trajectories on the effective quantum potential. The equation of motion for the spatial coordinates of the system and bath are

$$\dot{x} = \frac{-\partial V_{\text{eff}}}{\partial x} = -4A_{\text{eff}}x^3 + 2B_{\text{eff}}x^2 + m\sum_{j=1}^{N} c_j\omega_j^2(y_j - c_j x) \tag{14a}$$

$$\dot{y}_j = \frac{-\partial V_{\text{eff}}}{\partial y_j} = -m\omega_j^2(y_j - c_j x) \tag{14b}$$

The initial value of the momentum conjugate to the hydrogen bond coordinate, p_x, and the initial values of the bath phase space variables, $\{\vec{y}_o, \vec{p}_{yo}\}$, are sampled from the weight $e^{-\beta H_{\text{eff}}(x_0=0, p_{xo}, \vec{y}_o, \vec{p}_{yo})}$ via the Box-Muller algorithm.[19] The trajectories are performed with the leapfrog Verlet algorithm,[20] and we find 10 000 trajectories are enough to converge all results.

In Figure 1 we show the classical rate constants vs friction strength for proton transfer across a barrier of 15 kJ mol^{-1}. The results for the fast and slow frictions are shown in panels (a) and (b), respectively. As mentioned above the system exhibits the Kramers turnover behavior. We observed similar behavior for the larger barrier height of 95 kJ mol^{-1}.

In Figure 2(a) we show the effective and classical potentials for the slow friction at two different values of the friction strength for the strongly hydrogen bonded system. The solid line is the classical potential, the short dashed line is the effective quantum potential for a strong friction of $f = 5 \times 10^{-5}$ a.u. (after the turnover region), and the long dashed line is for weak friction of $f = 1 \times 10^{-5}$ a.u. This figure demonstrates that the effective quantum potential gets nearer to the original classical potential in the strong friction regime. Thus the quantum kinetic isotope effect should be diminishing in the large friction regime. We have found that this trend holds true as the barrier height increases, and thus the strength of the hydrogen bond decreases.

In Figure 2(b) we show the effective and classical potentials for a friction strength of $f = 5 \times 10^{-5}$ a.u. at two

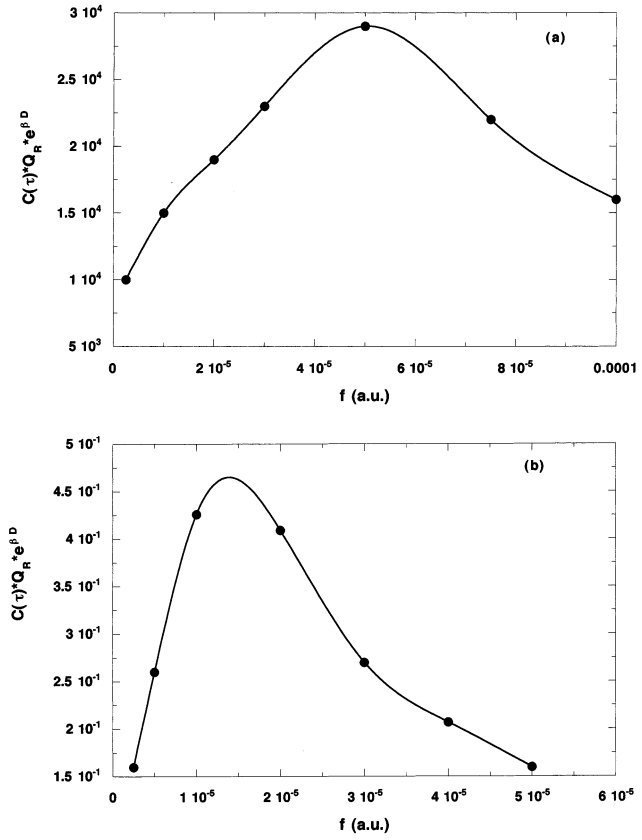

Figure 1. Classical value of the rate constants as a function of friction strength for the two friction time scales studied in this work. Panel (a) is for the slow friction response and panel (b) is for the faster friction.

different values of the friction time scale for the strongly hydrogen bonded system. The solid line is the classical potential, the short dashed line is the effective quantum potential for fast friction ($\sigma = 800$ fs), and the long dashed line is for slow friction ($\sigma = 3000$ fs). This figure demonstrates that the effective quantum potential gets nearer to the original classical potential in the faster solvent response regime. Thus the quantum kinetic isotope effect should be diminishing as the solvent response time increases.

In Tables 1−4 we show the rate constant ratios for deuteron to proton transfer for the two barrier heights studied at various friction strengths and time scales. Tables 1 and 3 show that the rate constant ratio is on the order of 10^{-1} for the LBHB (barrier height of 15 kJ mol^{-1}) over a wide spectrum of friction strengths and time scales. Tables 2 and 4 show that the weaker hydrogen bonded system (barrier height of 95 kJ mol^{-1}) have much smaller values of the rate constant ratio ranging from $10^{-6}-10^{-4}$. Thus, there is a significant kinetic isotope effect that can be used to differentiate between weak and strong hydrogen bonded systems. The strongly hydrogen bonded systems have a rate constant ratio of deuteron to proton transfer ranging from 3−6 orders of magnitude larger than the weakly hydrogen bonded system at a given friction strength and time scale. The origin of this large isotope effect is due to the large difference between the ability of the proton and deuteron to tunnel through the barrier. The tunneling corrections become particularly important as the barrier height increases, and this large isotope effect is consistent (in order of magnitude) with a simple analytic expression that has been derived by others.[23]

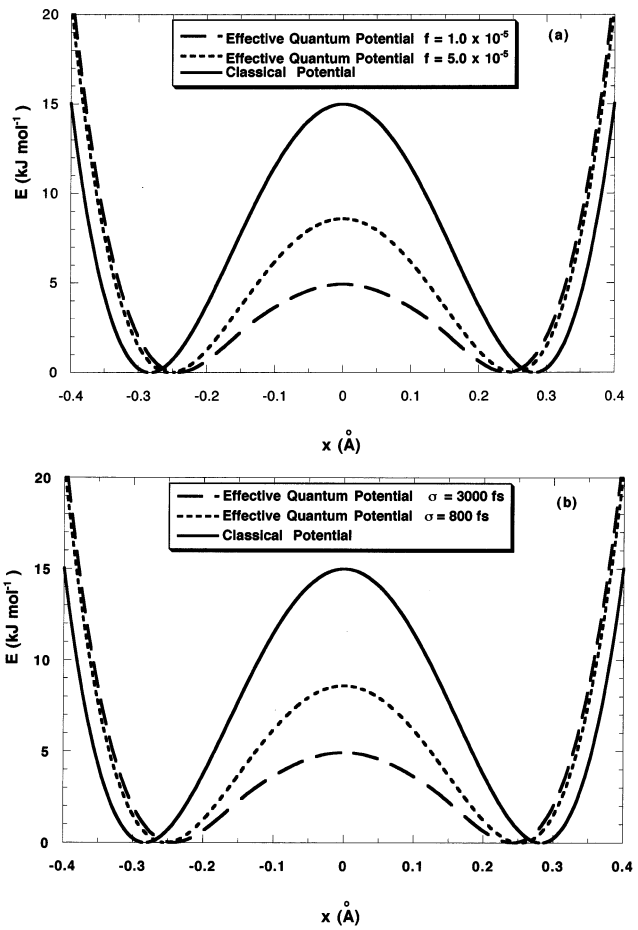

Figure 2. The effective quantum potentials. Panel (a) shows the classical (solid line) and effective quantum potentials for friction strengths of $f = 1 \times 10^{-5}$ a.u. (long dashed line) and $f = 5 \times 10^{-5}$ a.u. (short dashed line). The friction time scale is $\sigma = 800$ fs. Panel (b) shows the classical (solid line) and effective quantum potentials for friction time scales of $\sigma = 800$ fs (short dashed line) and $\sigma = 3000$ fs (long dashed line). The friction strength is $f = 5 \times 10^{-5}$ a.u.

Table 1. Barrier Height = 15 kJ mol^{-1} and $\sigma = 800$ fs

friction strength	φ	$e^{-\beta(D^D_{\text{eff}}-D^H_{\text{eff}})}$	$\left(\frac{\langle\chi_{\text{eff}}\rangle_D}{\langle\chi_{\text{eff}}\rangle_H}\right)$	$\left(\frac{\kappa_D}{\kappa_H}\right)$
2.00×10^{-5}	2.5	0.17	1.0	0.07
3.00×10^{-5}	2.5	0.21	1.3	0.11
4.00×10^{-5}	2.4	0.29	0.6	0.08
5.0×10^{-5}	2.4	0.33	0.8	0.11

Table 2. Barrier Height = 95 kJ mol^{-1} and $\sigma = 800$ fs

friction strength	φ	$e^{-\beta(D^D_{\text{eff}}-D^H_{\text{eff}})}$	$\left(\frac{\langle\chi_{\text{eff}}\rangle_D}{\langle\chi_{\text{eff}}\rangle_H}\right)$	$\left(\frac{\kappa_D}{\kappa_H}\right)$
2.00×10^{-5}	7.5	1.2×10^{-5}	0.9	1.5×10^{-6}
3.00×10^{-5}	7.0	6.7×10^{-5}	0.7	6.2×10^{-6}
4.00×10^{-5}	6.7	5.6×10^{-3}	0.5	3.8×10^{-4}
5.0×10^{-5}	6.4	1.1×10^{-2}	0.5	8.3×10^{-4}

There are two trends for the rate constant ratios in the weakly hydrogen bonded system. First, as the friction strength increases in both the slow and fast friction regimes the rate constant ratio increases. This means the kinetic isotope effect is diminishing as a function of increased friction strength. This can be explained from Figure 2(a), which shows that the effective quantum potential gets closer

Table 3. Barrier Height = 15 kJ mol^{-1} and σ = 3000 fs

friction strength	φ	$e^{-\beta(D^D_{\text{eff}}-D^H_{\text{eff}})}$	$\left(\frac{\langle\chi_{\text{eff}}\rangle_D}{\langle\chi_{\text{eff}}\rangle_H}\right)$	$\left(\frac{\kappa_D}{\kappa_H}\right)$
3.0×10^{-5}	2.6	0.18	1.5	0.10
5.0×10^{-5}	2.6	0.17	1.1	0.07
8.0×10^{-5}	2.5	0.18	1.1	0.08
1.0×10^{-4}	2.5	0.27	1.1	0.12

Table 4. Barrier Height = 95 kJ mol^{-1} and σ = 3000 fs

friction strength	φ	$e^{-\beta(D^D_{\text{eff}}-D^H_{\text{eff}})}$	$\left(\frac{\langle\chi_{\text{eff}}\rangle_D}{\langle\chi_{\text{eff}}\rangle_H}\right)$	$\left(\frac{\kappa_D}{\kappa_H}\right)$
3.0×10^{-5}	8.1	7.1×10^{-6}	2.2	1.9×10^{-6}
5.0×10^{-5}	7.8	9.5×10^{-6}	1.9	2.4×10^{-6}
8.0×10^{-5}	7.3	2.9×10^{-5}	1.2	4.8×10^{-6}
1.0×10^{-4}	7.1	1.8×10^{-4}	0.7	1.7×10^{-5}

Table 5. Friction Strength = 5×10^{-5} and σ = 800 fs

barrier height (kJ mol^{-1})	φ	$e^{-\beta(D^D_{\text{eff}}-D^H_{\text{eff}})}$	$\left(\frac{\kappa_D}{\kappa_H}\right)$
10	2.0	0.30	0.15
20	2.9	0.14	4.6×10^{-2}
40	4.4	0.02	4.1×10^{-3}
60	5.6	7.8×10^{-4}	1.4×10^{-4}
80	7.2	1.0×10^{-5}	1.5×10^{-6}

Table 6. Friction Strength = 3×10^{-5} and σ = 3000 fs

barrier height (kJ mol^{-1})	φ	$e^{-\beta(D^D_{\text{eff}}-D^H_{\text{eff}})}$	$\left(\frac{\kappa_D}{\kappa_H}\right)$
10	1.9	0.24	0.13
20	3.0	0.08	2.7×10^{-2}
40	4.8	7.7×10^{-3}	1.6×10^{-3}
60	6.1	2.4×10^{-4}	4.0×10^{-5}
80	7.8	5.1×10^{-6}	6.6×10^{-7}

the classical potential as the friction strength increases. The second trend is that the rate constant ratios are smaller in the slow friction regime than in the fast friction regime. This means that the kinetic isotope effect diminishes as the friction time scale increases. This can be explained from Figure 2(b), which shows that the effective quantum potential gets closer to the classical potential as the friction response time increases.

As seen by the third column in the tables the dynamical component of the rate constant, i.e., the ($\langle\chi_{\text{eff}}\rangle_D/\langle\chi_{\text{eff}}\rangle_H$) term in eq 12, does not have a large effect on the rate constant ratio. Thus we estimate the rate constant ratio from the thermodynamic contribution, i.e.,

$$\frac{\kappa_D}{\kappa_H} \approx \frac{e^{-\beta(D^D_{\text{eff}}-D^H_{\text{eff}})}}{\varphi} \tag{15}$$

In Tables 5 and 6 we show the rate constant ratios using eq 15 for a range of barrier heights at moderate friction strength for the two friction time scales, σ = 800 fs (Table 5) and σ = 3000 fs (Table 6). As shown by the tables at barrier heights above 20 kJ mol^{-1} the rate constant ratio is $< 10^{-3}$, while below 20 kJ mol^{-1} this ratio is $> 10^{-2}$.

These results show that there is a significant kinetic isotope effect on the transfer rate between donor and acceptor sites in a hydrogen bond. This effect, although perhaps easy to predict a priori, is quite complex in its details. The isotope effect found here depends very strongly on the characteristics of the surrounding solvent if the hydrogen bond is weak. If the hydrogen bond is strong (a LBHB), then the isotope effect depends very weakly on the solvent characteristics. For example, the isotope effect varies by as much as 2 orders of magnitude with friction strength for the weak hydrogen bond. By contrast, the LBHB shows the about the same value of the rate constant ratio (κ_D/κ_H) for all friction strengths and time scales studied.

IV. CONCLUSION

Our goal in this paper was 2-fold. First, to present an approximate way to compute rate constants for proton transfer in a hydrogen bonded system in the presence of a solvent. We did this by computing the classical reactive flux on an effective quantum mechanical potential. The idea of propagating classical trajectories on an effective quantum mechanical surface is not a new idea, but recently, several workers have presented a more rigorous approach to this idea.[21,22] The approach taken in this paper was derived in a previous work, where it was shown to be very accurate when compared to exact calculations of the rate constant.[12] In this work we have shown how to apply this technique to hydrogen bonded systems in the presence of a solvent.

The second goal of this work was to quantify the expected kinetic isotope effects for proton transfer in a strongly hydrogen bonded system. We have found that the dynamical component of the isotope effect is negligible (i.e., on the order of unity), and all the important isotope effects come from two thermodynamic factors. These are the activation energy and isotopic fractionation factor. Again, one might have predicted beforehand that the dynamics would play a small role in the kinetic isotope effects in a hydrogen bonded system. In this work we have quantified this statement. We have found that for a LBHB the ratio of deuteron to proton transfer is on the order of 10^{-1} for barriers below 15 kJ mol^{-1}, regardless of the friction strength and friction time scale. For weak, high barrier hydrogen bonds, this ratio of proton-transfer rates is on the order of 10^{-6} in the weak friction regime and 10^{-4} in the stronger friction regime. This is an extremely large isotope effect. This large isotope effect is due to the large difference between the ability of the proton and deuteron to tunnel through the barrier. In fact, this large isotope effect is consistent (in order of magnitude) with a simple analytic expression that has been derived by others.[23]

ACKNOWLEDGMENT

M. Messina would like to acknowledge the support from the donors of the Petroleum Research Fund, administered by the ACS.

REFERENCES AND NOTES

(1) Cleland, W. W.; Kreevoy, M. M. Low-barrier hydrogen bonds and enzymic catalysis. *Science* **1994**, *264*, 1887−1890.

(2) Guthrie, J. P. Short strong hydrogen bonds: can they explain enzymic catalysis? *Chem. Biol.* **1996**, *3*, 163−170.

(3) Frey, P. A.; Whitt, S. A.; Tobin, J. B. A low-barrier hydrogen bond in the catalytic triad of serine proteases. *Science* **1994**, *264*, 1927−1930.

(4) Neidhart, D.; Wei, Y.; Cassidy, C.; Lin, J.; Cleland, W. W.; Frey, P. A. Correlation of low-barrier hydrogen bonding and oxyanion binding in transition state analogue complexes of chymotrypsin. *Biochemistry* **2001**, *40*, 2439−2447.
(5) Shan, S.; Herschlag, D. The change in hydrogen bond strength accompanying charge rearrangement. Implications for enzymic catalysis. *Proc. Natl Acad. Sci. U.S.A.* **1996**, *93*, 14474−14479.
(6) Cassidy, C.; Lin, J.; Frey, P. A. A new concept for the mechanism of action of chymotrypsin: the role of the low barrier hydrogen bond. *Biochemistry* **1997**, *36*, 4576−4584.
(7) Kreevoy, M. M.; Liang, T. M. Structures and isotopic fractionation factors of complexes, $A_1HA_2^-$. *J. Am. Chem. Soc.* **1980**, *102*, 3315−3322.
(8) Lin, J.; Westler, W. M.; Cleland, W. W.; Markley, J. L.; Frey, P. A. Fractionation factors and activation energies for exchange of the low barrier hydrogen bonding proton in peptidyl trifluoromethyl ketone complexex of chymotrypsin. *Biochemistry* **1998**, *95*, 14664−14668.
(9) Speakman, J. C. The crystal structures of the acid salts of some monobasic acids. *J. Am. Chem. Soc.* **1949**, 3357−3356.
(10) Altman, L. J, Laungani, D.; Gunnasson, G.; Wennerstrom, H.; Forsen, S. Proton, deuterium, and tritium nuclear magnetic resonance of intramolecular hydrogen bonds. Isotope effects and the shape of the potential energy function. *J. Am. Chem. Soc.* **1978**, *100*, 8264−8266.
(11) Hazdi, D. Infrared spectra of strongly hydrogen bonded systems. *Pure Appl. Chem.* **1965**, *11*, 435−453.
(12) Schenter, G. K.; Messina, M.; Garrett, B. C. Centroid-Density quantum rate theory. Dynamical recrossings of the dividing surface. *J. Chem. Phys.* **1993**, *99*, 1674−1683.
(13) Hanggi, P.; Talkner, P.; Borkovec, M. Reaction-rate theory: fifty years after Kramers. *Rev. Mod. Phys.* **1990**, *62*, 251−341.
(14) Chandler, D. Statistical mechanics of isomerization dynamics in liquids and the transition state approximation. *J. Chem. Phys.* **1978**, *68*, 2959−2970.
(15) Ventura, K. M.; Greene, S. N.; Halkides, C. J.; Messina, M. A mixed quantum-classical approach for computing effects of intramolecular motion on the low-barrier hydrogen bond. *Struct. Chem.* **2001**, *12*, 23.
(16) McRae, R. P.; Schenter, G. K.; Garrett, B. C.; Haynes, G. R.; Voth, G. A.; Schatz, G. C. Critical comparison of approximate and accurate quantum- mechanical calculations of rate constants for a model activated reaction in solution. *J. Chem. Phys.* **1992**, *97*, 7392.
(17) Messina, M.; Schenter, G. K.; Garrett, B. C. Approximate path integral methods for partition functions. *J. Chem. Phys.* **1993**, *98*, 4120−4127.
(18) Skodje, R. T.; Truhlar, D. G. *J. Chem. Phys.* **1981**, *85*, 624.
(19) Press, W. H.; Teukolsky, S. A.; Vetterling, W. T.; Flannery, B. P. *Numerical recipes in Fortran 77*; Cambridge University: New York, 1992.
(20) Allen, M. P.; Tildesley, D. J. *Computer simulation of liquids*; Oxford: 1987.
(21) Sagnella, D. E.; Cao, J.; Voth, G. A. A Semiclassical Reactive Flux Method for the Calculation of Condensed Phase Activated Rate Constants. *Chem. Phys*. **1994**, *180*, 167−180.
(22) (a) Cao, J.; Voth, G. A. The Formulation of Quantum Statistical Mechanics Based on the Feynman Path Centroid Density. II. Dynamical Properties. *J. Chem. Phys.* **1994**, *100*, 5106−5117. (b) Cao, J.; Voth, G. A. The Formulation of Quantum Statistical Mechanics Based on the Feynman Path Centroid Density. III. Phase Space Formalism and Analysis of Centroid Molecular Dynamics. *J. Chem. Phys*. **1994**, *101*, 6157−6167. (c) Cao, J.; Voth, G. A. The Formulation of Quantum Statistical Mechanics Based on the Feynman Path Centroid Density. IV. Algorithms for Centroid Molecular Dynamics. *J. Chem. Phys*. **1994**, *101*, 6168−6183.
(23) Hänggi, P.; Grabert, H.; Ingold, G.; Weiss, U. Quantum Theory of Activated Events in the Presence of Long-Time Memory. *Phys. Rev. Lett.* **1985**, *55*, 761.

CI0203444